International Journal of Mass Spectrometry 216 (2002) 75–83
www.elsevier.com/locate/ijms

Reverse field technique to study delayed ionization in time-of-flight mass spectrometry

J.R. Stairs, A.W. Castleman Jr.*

152 Davey Laboratory, Departments of Chemistry and Physics, The Pennsylvania State University, University Park, PA 16802-7003, USA

Received 9 November 2001; accepted 22 January 2002

Abstract

Delayed ionization has been observed following the photoexcitation of cluster systems (i.e., fullerenes, Met-Cars, refractory metal clusters, etc.) where the ionization potential is lower than the binding energy of the cluster. A reverse field technique to study delayed ionization is presented herein which enables the details of the mechanism to be investigated in selected time intervals following the photoexcitation process. (Int J Mass Spectrom 216 (2002) 75–83) © 2002 Elsevier Science B.V. All rights reserved.

Keywords: Clusters; Met-Cars; Delayed ionization; Thermionic emission

1. Introduction

Since the discovery of the family of metallocarbohedrenes (Met-Cars) by our group in the early nineties [1,2], many interesting phenomena have been observed. Possibly, one of the most exiting characteristics of the Met-Car family is delayed ionization. Since first observations of delayed ionization [3,4], attempts have been made to describe the mechanism in terms of the thermionic emission model developed for electron emission from bulk metals [5,6]. The thermionic emission model was adapted by Klots to account for systems of finite size [7]; however, according to Campbell and Levine [8], evidence is accumulating that delayed ionization can also depend on the time-scale and means of excitation. Stimulated by our findings of extensive delayed ionization in Met-Cars and growing interest in the basic mechanisms, we developed a method of studying the details of the process in selected short time intervals.

In previous experiments, delayed ionization was measured with an altered Wiley–McLaren time-of-flight (TOF) lens assembly (see Fig. 1) where the molecular beam was directed parallel to the axis of detection [5,9]. In order to prevent prompt ions from being detected, a blocking field was applied to the source region for a finite time after the ionization laser interacted with the molecular beam. The blocking field was then removed, resulting in a field free region between the reflector plate, R, and the extractor plate, E, until at some fixed time later (∼3 μs) an extraction pulse was applied to accelerate the delayed ions toward the detector.

The method described here involves a reverse extraction field applied perpendicular to the excited molecular beam. Since this method extracts the ions orthogonal to the molecular beam and eliminates the field free region between the extraction and repeller

* Corresponding author. E-mail: awc@psu.edu

PII S1387-3806(02)00550-X

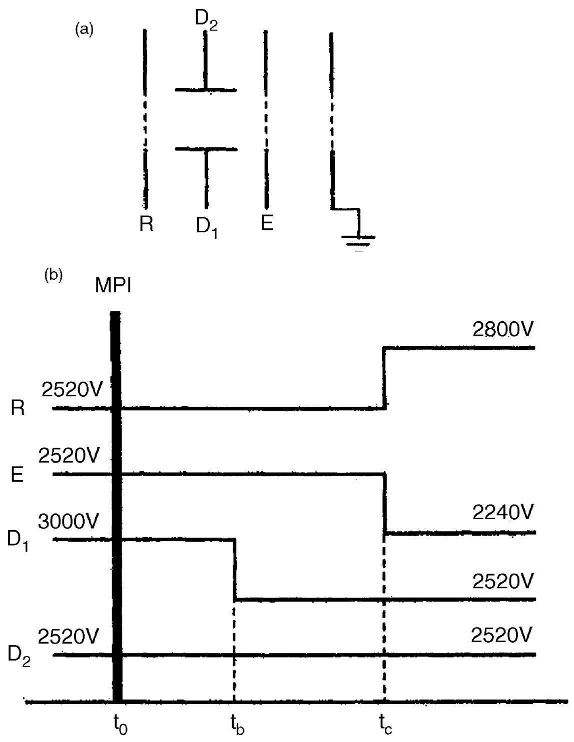

Fig. 1. (a) Altered Wiley–McLaren time-of-flight set-up used in prior technique to study delayed ionization. (b) Potential difference between D_1 and D_2 "block" prompt ions from detection until time, t_b, while no potential difference exists between R (TOF_1) and E (TOF_2). Then, after t_b, a FFR exists until the extraction time, t_e, when the voltage on R pulses up and the voltage on E pulses down to accelerate the ions to the detector.

plate (TOF_1 and TOF_2, respectively), the mass resolution is increased enabling a more facile investigation of the electron emission rate in selected time intervals. The details of the technique are discussed herein, and new observations of delayed ionization observed through its implementation will be presented in a future publication.

2. Experimental

A reflectron time-of-flight mass spectrometer (R-TOFMS) equipped with a laser vaporization (LaVa) source was employed to study delayed ionization (Fig. 2). The LaVa source consisted of a rotating and translating 6.35 mm diameter zirconium rod (99.9% purity, Aldrich) which was laser ablated using the second harmonic (532 nm) of a Nd:YAG laser (Spectra Physics GCR-150) focused by a lens of 70 cm focal length. A mixture of 15% CH_4/He ultra-high purity gas was pulsed through a nozzle (General valve 99-43-900; a modified version of a standard General Valve Series 9 with short pulse duration [10]) with a backing pressure of 4.9×10^3 Torr over the metal rod at the point of ablation. The mixed vapor was then supersonically expanded into the source chamber at a pressure of 6×10^{-5} Torr to form zirconium carbide clusters. In order to study only neutral species, ions created in the plasma of the LaVa source were prevented from reaching the ionization region by use of a deflection rod located approximately 10 cm from the source, to which was applied a potential of ~275 V. The molecular beam was then skimmed and an Excimer XeCl laser (308 nm, Lambda Physik EMG 201 MSC) with a pulse width of ~10 ns was used to ionize the Zr_xC_y species. The power of the Excimer laser was measured to be 9.46 mJ per pulse at the Brewster's window. In this set-up, the molecular beam was perpendicular to the axis of detection for increased mass resolution and only cations were detected. The pressure of the detection chamber was 9×10^{-7} Torr. The source chamber and detection chamber were pumped with a total of four Alcatel oil diffusion pumps backed by mechanical pumps.

In order to remove the prompt ions and observe the delayed ion species, a fast high voltage transistor switch (Behlke switch, Eurotek, Inc., USA) was used to pulse the voltage, U_1, on TOF_1 from 3000 to 4500 V (see Fig. 3). The Behlke switch possesses a rise time of ~30 ns and a total fall time of ~75 μs. The voltage, U_2, on TOF_2 (see Fig. 4), was held constant at 4125 V so that initially, before TOF_1 was pulsed to 4500 V, there is an electric field that accelerates the prompt ions away from the detector towards TOF_1 where they are made undetectable as they collide with TOF_1 [11].[1] At some variable delay time, Δt, after

[1] Although this technique is similar to that used by Hertel and co-workers [11] the use of the fast high voltage transistor Behlke switch, allows one to observe events that occur on a faster time-scale than what Hertel and co-workers were able to study.

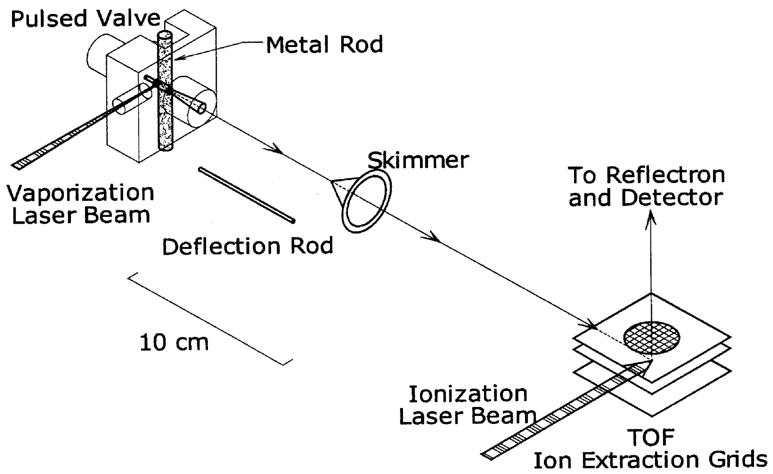

Fig. 2. Schematic of ion source for R-TOFMS.

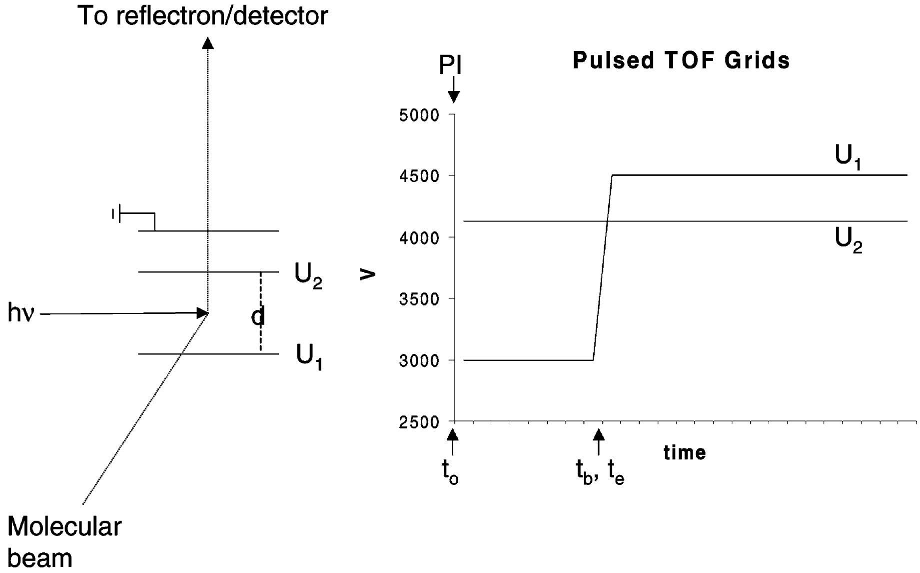

Fig. 3. New technique to study delayed ionization. From t_0 to t_b, the potential on TOF$_1$, U_1, is 3000 V and the potential, on TOF$_2$, U_2, is 4125 V causing ions created in that time to be accelerated into TOF$_1$. Then, at t_e, U_1 pulses up to 4500 V and ions created after that time are accelerated towards the detector. Notice that in the new technique, t_b and t_e are approximately the same time.

the ionization laser interacts with the molecular beam, the voltage on TOF$_1$ was pulsed to 4500 V. The voltage of TOF$_1$ was higher than TOF$_2$ for approximately 48 μs so that any delayed ions created after the voltage on TOF$_1$ was pulsed were accelerated towards a reflectron and then a microchannel plate (MCP) detector (Galileo).

TOF$_1$ was separated from TOF$_2$ by 1.35 cm and TOF$_2$ was separated from TOF$_3$, which was grounded, by 0.7 cm. There was then a field free region (FFR),

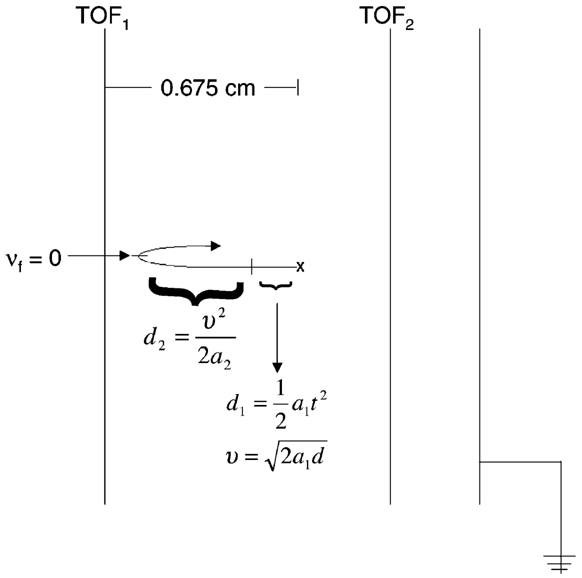

Fig. 4. Schematic of the TOF acceleration region. X is the point at which the ionization laser interacts with the molecular beam. The curved arrow represents the path of the ion that theoretically does not get accelerated into TOF_1. The first bar across the ion path represents the point at which the U_1 pulses from 3000 to 4500 V. At this point, the ion has to slow down, stop (at the second bar where $v = 0$) and turn around. The calculations represent the distance the ion travels during these two segments of the ion path. If $d_1 + d_2 \geq 0.675$ cm, then the ion collides with TOF_1.

1.275 m, which leads to the first grid of the reflectron. The first grid of the reflectron was grounded and separated from the second grid of the reflectron, held at a potential of ~3000 V, by 1.5 cm. There was then 10.8 cm separating the second grid from the third and final grid of the reflectron, which was held at a potential of ~4900 V. After the reflectron, ions traversed a second FFR, 0.4 m, followed by the MCP detector.

The entire system runs at 30 Hz. Data is collected and averaged over 300 scans on a digital oscilloscope (Link Instruments, DSO-2100).

3. Discussion

In order to theoretically determine whether or not the electric field needed to remove the prompt ions would be effective and whether or not the technique presented here was practical, a simple calculation utilizing the kinematic equations was performed. As mentioned above, the distance between TOF_1 and TOF_2 is 1.35 cm. With U_1 at 3000 V and U_2 at 4125 V, a potential difference of 1125 V was created giving rise to an electric field of −833.3 V/cm (the negative sign is inserted here to represent the field's direction for cations towards TOF_1). Since $F = Eq = ma$, the acceleration specific to individual masses can be calculated, where E is equal to 833.3 V/cm. The time interval, Δt, between the instant when the ionizing laser interacts with the molecular beam and when U_1 is pulsed can be changed by increments of 0.05 μs. Using the time interval for which the field is −833.3 V/cm, and the acceleration determined from the field (a_1), the distance that the mass will travel towards TOF_1 can be determined (see Fig. 4). If that distance is greater than half of the distance between TOF_1 and TOF_2 (0.675 cm), assuming that the ions are created at the half-way point between these two grids, then the ions will collide with TOF_1 and will not be detected. Notice in Fig. 4 that a_1 represents the acceleration before TOF_1 pulses ($U_1 = 3000$ V) and a_2 is the acceleration after TOF_1 pulses ($U_1 = 4500$ V).

Hence, after substitution of the values stated above and 0.05 and 0.1 μs for t, masses up to 447 amu are calculated to be removed in the first time increment while masses up to 1788 amu will be removed by the second time increment. Also, keep in mind that these calculations were done with the assumption that the ions are created at the half-way point between TOF_1 and TOF_2. In actuality, the ionization point was more likely closer to TOF_1. While preparing for the experiment, the ionization laser was lowered until it was confirmed through observation of an enormous baseline jump on the oscilloscope, that the ionization laser was striking TOF_1. The ionization laser was then elevated until adequate Zr_xC_y signal was achieved, therefore placing the ionization event as close to TOF_1 as possible, and decreasing the time it takes for ions to travel the distance to collide with TOF_1. Through these calculations it can be seen that theoretically, the method is valid.

4. Results

Delayed ionization studies were carried out on zirconium carbide clusters including the Met-Car, Zr_8C_{12} (see Fig. 5 for a spectrum taken with no time delay). The delay between the laser pulse interacting with the molecular beam and the pulsing of U_1 was increased for the majority of the experiment in increments of 0.05 μs. At times when all clusters were absent from the spectra and only the delayed atomic ion remained, steps of 0.20 μs were taken (see Fig. 6).

After integrating the area under the peaks of the Met-Car, the atomic ion, Zr^+ (which is seen to undergo a substantial delayed emission process) and a peak with $m/z \sim 27$, the resulting intensity was plotted vs. the delay time (Fig. 7). Several things can be seen from Fig. 7. It is evident from the spectra that the marker peak (which is most likely an impurity in the methane) has no delayed ionization. The intensity for this peak is constant and within one 0.05 μs increment, the intensity falls to zero (see Fig. 7). Since methane impurity has no delayed ionization, the last point in time at which this peak has a detectable intensity is considered to be time zero, t_0. That is, t_0 is considered to be the point at which the ionization laser is interacting with the molecular beam at the same time that U_1 is pulsing and accelerating ions towards detection. For this reason, the peak with $m/z \sim 27$ is referred to as the marker peak.

Also at this time, peaks with m/z 1, 4, and 14–16 display anomalous behaviors as can be seen in Fig. 8. At the same range of time at which the marker peak is no longer detected, the referred to peaks appear to develop daughter peaks that are detected at slightly earlier times. These so-called daughter peaks then dominate the spectrum as the "parent" peaks disappear. We believe that these daughter peaks are a result of the prompt ions that are accelerated towards TOF_1.

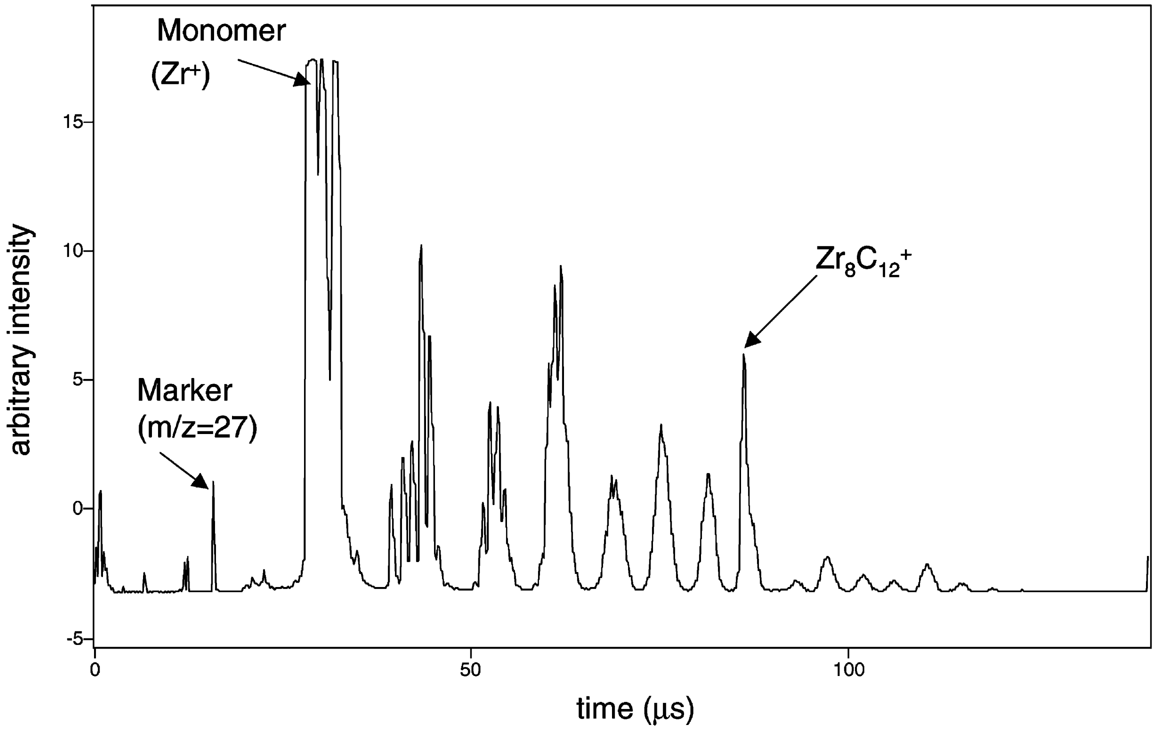

Fig. 5. Time-of-flight mass spectrum showing the $m/z \sim 27$ "marker" peak, the zirconium monomer (Zr^+) and the Met-Car ($Zr_8C_{12}{}^+$). Spectrum was taken with $U_1 = 4500$ V and $U_2 = 4125$ V.

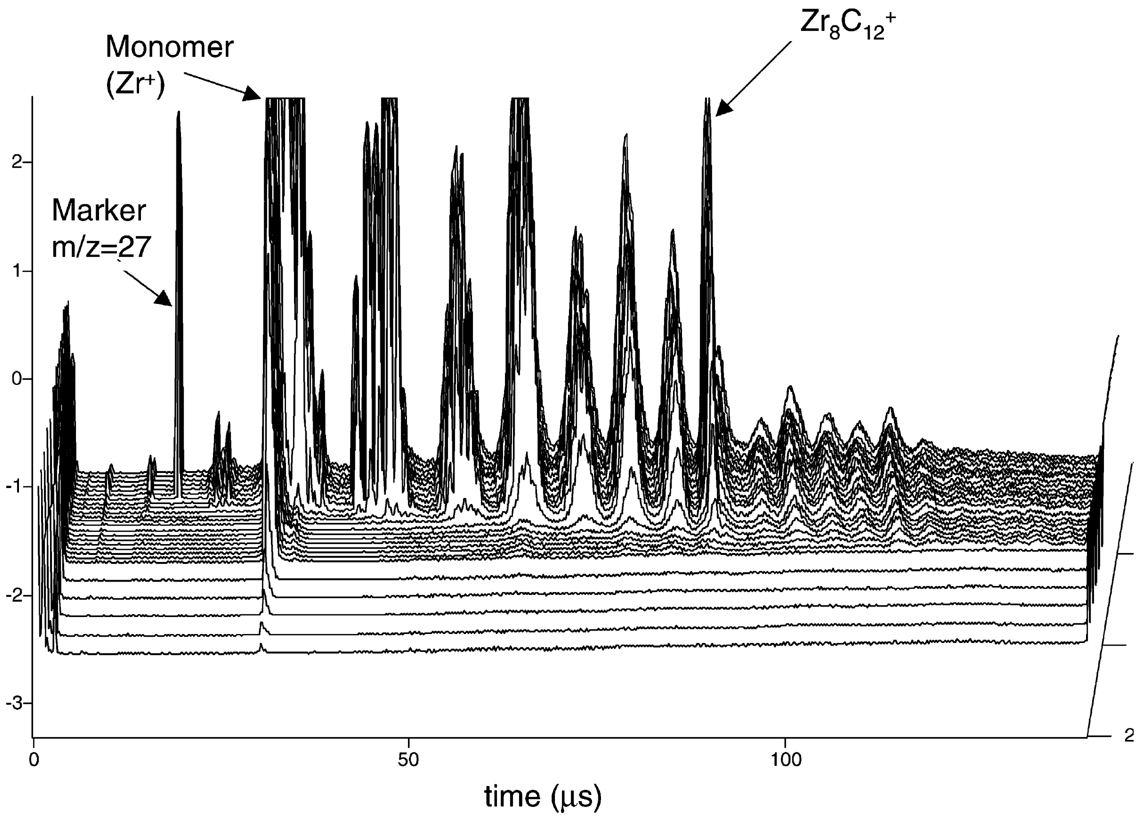

Fig. 6. 3-D plot of zirconium carbide clusters spectra at increasing delay time from top to bottom (0.05, 0.20 μs steps). The last spectrum displaying the marker peak is the zero time. Note the long delay of the Met-Car and the atomic ion, Zr^+.

These prompt ions that experience the "backward" field crash into TOF_1. That ensuing impact ejects particles that were adsorbed onto TOF_1. When U_1 pulses to send ions towards the detector, these ejected particles are "born" at TOF_1. Since they are born at TOF_1, they possess a higher birth potential (BP) as they are accelerated towards the detector. From this higher BP, the ejected particles accrue a higher kinetic energy and therefore reach the detector at a slightly earlier time. The ejected particles represented by the daughter peaks then dominate the spectrum because the prompt ions themselves are no longer being detected but are crashing into TOF_1. The time at which the daughter peaks dominate the spectrum and the parent peaks disappear, coincide with the time at which the marker peak is no longer detected. This anomalous behavior further validates that the marker peak can be used experimentally to determine the t_0 in the delayed ionization experiments.

Once the zero time delay between the laser interaction with the molecular beam and the pulsing of TOF_1 was determined, an interpretation of the data collected by means of this technique was necessary and is as follows. At the t_0, the ionization laser interacts with the molecular beam at the same time that the voltage on TOF_1 pulses to 4500 V, therefore, prompt ions are detected. However, since TOF_1 possesses a potential higher than TOF_2 for ∼48 μs after the pulsing event, prompt ions as well as any delayed ions formed in that 48 μs time span are detected at t_0. Since delayed ionization commonly occurs in a few microseconds [3–9], 48 μs is ample time to sample all ions created

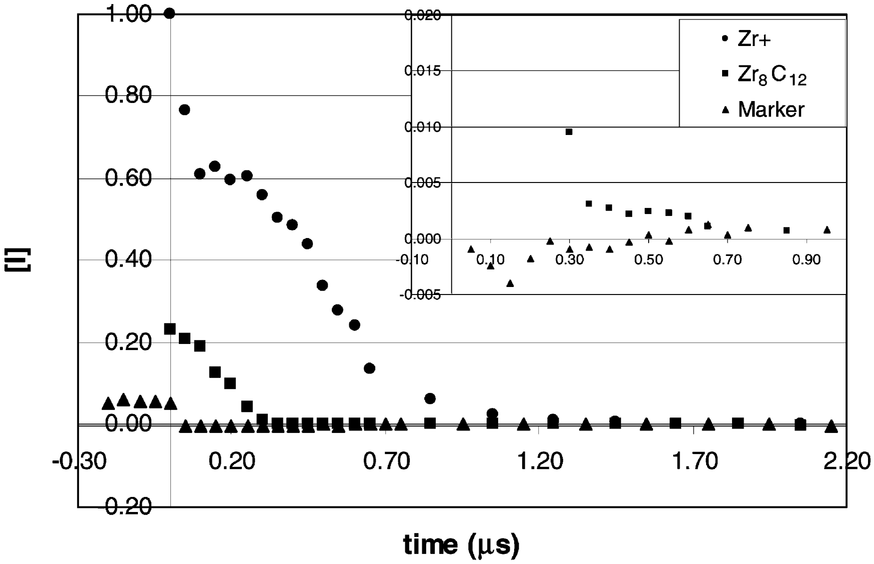

Fig. 7. Plot of normalized intensity vs. delay time for the marker peak, atomic ion and the Met-Car. Inset shows behavior of the Met-Car between 0.35 and 0.65 μs.

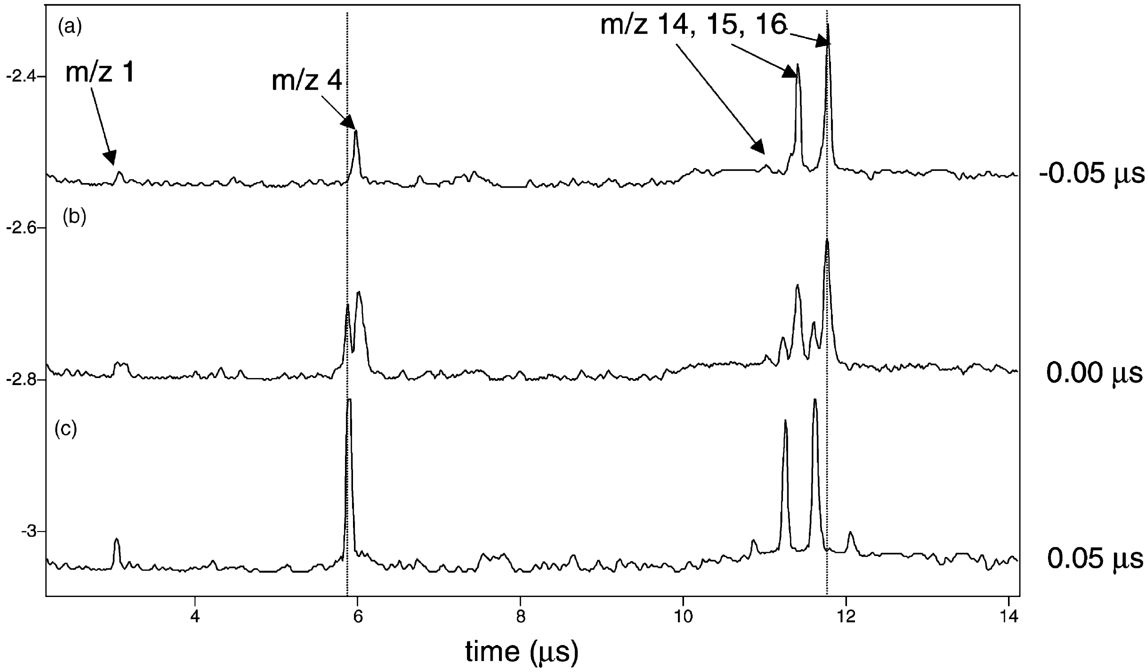

Fig. 8. (a) Peaks representing *m/z* 1, 4, and 14–16. (b) Satellite peaks grow into the spectrum as prompt ions collide with TOF_1 detaching species adsorbed onto TOF_1. When U_1 pulses from 3000 to 4500 V, these detached ionic species are then accelerated to the detector at higher kinetic energies causing them to appear in the spectrum slightly before their "parent" ions. (c) These satellite peaks dominate over the original parent peaks at the time delay when all prompt ions are accelerated into TOF_1. This happens at time 0.05 μs and coincides with the time when the marker peak is no longer detected.

after photoexcitation. The quantity of ions detected at time zero then represents the integral, or sum, of all ions created.

As the time at which TOF_1 pulses from 3000 to 4500 V is delayed, more ions are sent towards TOF_1 rather than the detector. Delaying the extraction time that accelerates the ions to the detector effectively removes any ions that were created in that 0.05 μs increment of time, thereby reducing the overall quantity of ions detected. If the difference in ion intensity from one delay time to its subsequent longer delay time is taken, then slices in time of the delayed ionization process can be studied. These data and their implications will be discussed in a future publication.

The plot in Fig. 7 shows that the Met-Car has a delayed ionization with a large decrease of intensity at 0.35 μs. With closer inspection (see inset in Fig. 7) it can be seen to have a finite intensity above the baseline until 0.65 μs. Interestingly, the atomic ion undergoes delayed ionization until 1.95 μs. Note the small crests and valleys in the data for the delayed atomic ion at early delay times. These features were reproducible from one month to the next and at different fluences (although at low fluences they disappear). These trends will be addressed in a later publication.

The delayed atomic ion was also observed by May et al. [9] and was proposed to have a connection to the presence of the Met-Car. These delayed ionization experiments were repeated with conditions altered to suppress the formation of the Met-Car as can be seen in Fig. 9. To prevent the formation of the Met-Car, 100% He was used rather than the 15% CH_4/He mixture that

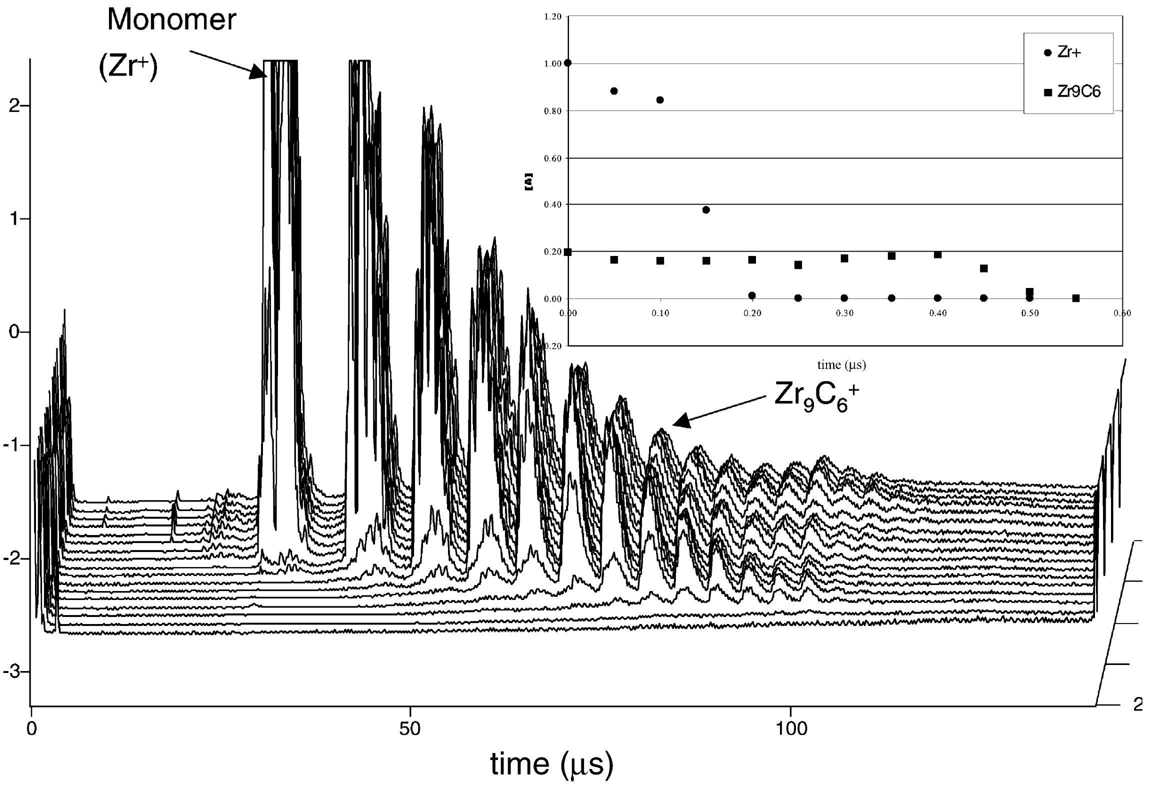

Fig. 9. Delayed ionization experiment with conditions set so that no Met-Cars are present. Notice that without Met-Cars present there is greatly reduced delayed atomic ion emission. Inset shows intensity of Zr^+ and $Zr_9C_6^+$ vs. delay time.

was used to produce the Met-Car.[2] When the Met-Car was not present, there was a drastic decrease in delayed atomic ion emission, providing experimental evidence for the earlier conjecture.

5. Conclusion

A technique to study delayed ionization was presented. The zirconium Met-Car, a species known to display delayed ionization, was investigated. Delayed ionization of the Met-Car and of the atomic ion was successfully observed and reported. A future publication will delve deeper into the intricacies of the data obtained using this technique and the phenomenon of delayed ionization.

Acknowledgement

The authors would like to thank AFOSR, Grant no. F49620-01-1-0122, for the financial support of this research.

[2] There was, however, still some carbon present on the zirconium rod which resulted in zirconium clusters that contained small amounts of carbon. As can be seen in Fig. 9, there is still a peak present approximately where the Met-Car would be observed, but slightly later in time. This peak corresponds to the Zr_9C_6 cluster ($m/z = 891$ amu). The inset plot in Fig. 9 represents the intensity of this peak vs. time delay. This peak shows interesting delayed ionization behavior. The intensity stays the same until $\sim$0.40 μs. Since, the potential on TOF_1 remains higher than that of TOF_2 for $\sim$48 μs after the pulse as described above, all ions that are born after the pulsing event are detected. Keeping this in mind one can see by the inset in Fig. 9 that no Zr_9C_6 ions are formed until $\sim$0.40 μs.

References

[1] B.C. Guo, K.P. Kerns, A.W. Castleman Jr., Science 255 (1992) 1411.
[2] B.C. Guo, S. Wei, J. Purnell, S. Buzza, A.W. Castleman Jr., Science 256 (1992) 515.
[3] P.D. Dao, A.W. Castleman Jr., J. Chem. Phys. 84 (1986) 1435.
[4] G.O. Neiman, E.K. Parks, S.C. Richtmeier, K. Liu, L.G. Pobo, S.R. Riley, High Temp. Sci. 22 (1986) 115.
[5] T. Leisner, K. Athanassenas, D. Kreisle, E. Recknagel, O. Echt, J. Chem. Phys. 99 (1993) 9670;
B.A. Collins, A.H. Amrein, D.M. Rayner, P.A. Hackett, J. Chem. Phys. 99 (1993) 4174.
[6] S.E. Kooi, A.W. Castleman Jr., J. Chem. Phys. 108 (1998) 8864.
[7] C.E. Klots, Chem. Phys. Lett. 186 (1991) 73.
[8] E.E.B. Campbell, R.D. Levine, Annu. Rev. Phys. Chem. 51 (2000) 65.
[9] B.D. May, S.F. Cartier, A.W. Castleman Jr., Chem. Phys. Lett. 242 (1995) 265.
[10] Y. Huang, M. Sulkes, Rev. Sci. Instrum. 65 (1994) 3868.
[11] E.E.B. Campbell, G. Ulmer, I.V. Hertel, Phys. Rev. Lett. 67 (1991) 1986.